Japanese Journal of Applied Physics
Vol. 43, No. 8B, 2004, pp. 5918–5921
©2004 The Japan Society of Applied Physics

High-Efficiency InGaAs/AlGaAs Quantum Well Distributed Bragg Reflector Laser with Curved Grating

Masahiro UEMUKAI, Kazutoshi KITANO, Naoyuki SHIMADA and Toshiaki SUHARA

Department of Electronic Engineering, Graduate School of Engineering, Osaka University, 2-1 Yamada-Oka, Suita, Osaka 565-0871, Japan

(Received January 19, 2004; accepted May 10, 2004; published August 25, 2004)

An InGaAs quantum well curved distributed Bragg reflector (DBR) laser designed for high efficiency and high wavelength purity operation is demonstrated. The laser was fabricated by a simple process without regrowth. In order to improve the performance, the quantum well was selectively disordered in the DBR grating region to accomplish low absorption loss. As a result of optimization of the curved DBR grating and low-reflection coating on the facet mirror, single-mode lasing with an external differential quantum efficiency as high as 0.74 and a side mode suppression ratio of 52 dB was achieved. Low noise characteristic of only 0.7 dB above the standard quantum limit was obtained. [DOI: 10.1143/JJAP.43.5918]

KEYWORDS: distributed Bragg reflector laser, semiconductor laser, quantum well laser, ridge structure laser, quantum well disordering, integrated optoelectronics

1. Introduction

Distributed Bragg reflector (DBR) lasers are attractive for many applications due to its advantages such as dynamic single mode lasing, high spectrum purity and precise wavelength control. The fabrication of DBR lasers usually requires epitaxial regrowth over a grating. Utilizing a surface grating eliminates the need for regrowth. In previous work, we proposed and demonstrated a quantum well DBR laser with a surface curved grating for reflecting a guided wave.[1] It is suitable for constructing monolithic integrated circuits, and monolithically integrated master oscillator power amplifier lasers for emitting a collimated output beam have been reported using the curved-DBR laser as a master oscillator.[2,3]

In order to improve the performance of the curved-DBR laser, a first-order DBR grating should be adopted instead of the third-order grating used in the previous work. Reduction of absorption loss in the DBR region is also one of the important requirements for implementing high-performance DBR lasers. This can be done by selective-area quantum well disordering by rapid thermal annealing with SiO_2 caps of different thicknesses.[4,5] To enhance external quantum efficiency and spectrum purity, the DBR grating must be optimized for both high reflectivity and sharp wavelength selectivity. Furthermore, low-reflection coating on a front facet would enhance the efficiency and improve catastrophic optical damage (COD) threshold level.

In this paper, we present design and fabrication of a high-efficiency quantum well DBR laser with a narrow active channel and a surface curved DBR grating. Quantum well disordering in the DBR region and low-reflection coating on the front facet are incorporated in the fabrication process. We demonstrate high-efficiency single-mode lasing with high spectrum purity of the curved-DBR laser.

2. Device Description and Design

The device is constructed with a narrow active channel and a surface curved DBR grating, as shown in Fig. 1. The narrow ridge structure ensures lateral single-mode operation, and the first-order curved DBR grating provides high reflectivity for the guided wave diverging from the end of the active channel. It was fabricated using an InGaAs/AlGaAs strained-layer single-quantum-well (QW) graded-index separate-confinement heterostructure (GRIN-SCH) waveguide,[6] shown in Fig. 2. It contains a 60-Å $In_{0.2}Ga_{0.8}As$ strained-layer QW as the active layer and a 100-Å GaAs high-index etch-stop layer inserted 0.1 µm above the top of the graded region. The QW is selectively disordered in the DBR grating region to accomplish low absorption loss.

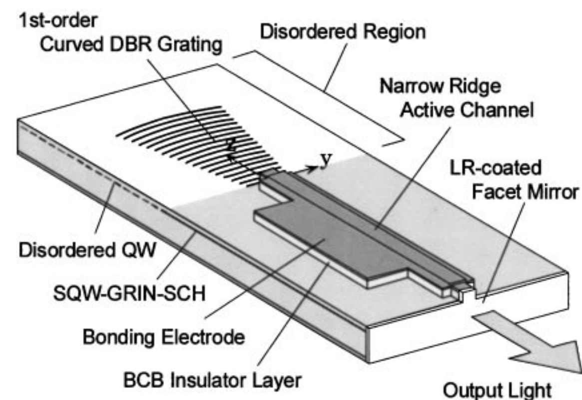

Fig. 1. Schematic of the high-efficiency DBR laser with curved grating.

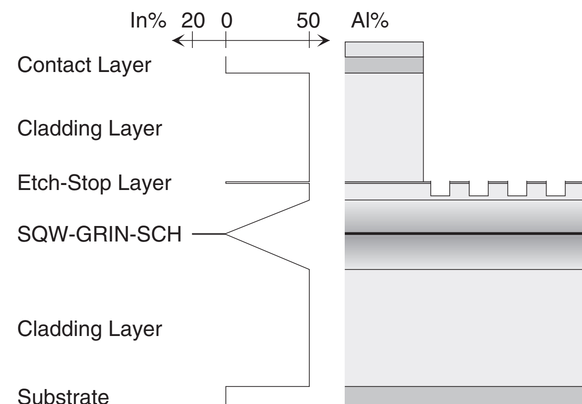

Fig. 2. Cross section of the SQW-GRIN-SCH waveguide/grating structure.

The first-order curved DBR grating was designed for a wavelength of 960 nm. The diverging guided wave can be approximated as a planar Gaussian beam with a waist width,

$2w_0$, corresponding to the $1/e^2$ width of the lateral mode profile at the end of the active channel. For a 2.0-μm ridge width, w_0 is calculated as 1.68 μm and the full divergence angle of the guided wave is 6.6°. The m-th line of the curved DBR grating pattern is determined by[1)]

$$2kz + \frac{kzy^2}{z^2 + (kw_0{}^2/2)^2} - \tan^{-1}\left(\frac{2z}{kw_0{}^2}\right) = 2m\pi, \quad (1)$$

where $k = 2\pi n_{\mathrm{eff}}/\lambda$, n_{eff} is the effective refractive index and λ the wavelength in free space. The coordinates y and z are indicated in Fig. 1.

The curved DBR grating for a length $L = 200$ μm was designed. By using selective area QW disordering, the absorption loss in the DBR grating region can be significantly reduced to $\alpha = 3\,\mathrm{cm}^{-1}$.[4)] The dependence of the DBR reflectivity R_{DBR} and the wavelength bandwidth $\Delta\lambda$ on the coupling coefficient κ was calculated for $L = 200$ μm and $\alpha = 3\,\mathrm{cm}^{-1}$. To obtain higher R_{DBR}, κ should be higher. On the other hand, κ should be lower for narrower $\Delta\lambda$. In order to obtain both high reflectivity and sharp wavelength selectivity, κ was determined as $130\,\mathrm{cm}^{-1}$. The corresponding groove depth was calculated as 70 nm. Using these values of κ and α, R_{DBR} and $\Delta\lambda$ were calculated as 96% and 1.6 nm, respectively.

By low-reflection (LR) coating of Al_2O_3 on the facet mirror, the external differential quantum efficiency η_d can be enhanced. LR coating can also enhance the COD threshold at the facet mirror. For the optimization, we used the internal loss of $3\,\mathrm{cm}^{-1}$, the internal differential quantum efficiency of 0.8, the differential gain of 0.035 cm/A and the transparency current density of 390 A/cm^2. These values were determined by preliminary experiment using the same epitaxial wafer. Using these values, η_d and the threshold current I_{th} were calculated for $R_{\mathrm{DBR}} = 96\%$ and a channel length of 600 μm. The dependence of η_d and I_{th} on the reflectivity of the facet mirror R_f is shown in Fig. 3. For a DBR laser without LR coating ($R_f = 29\%$), η_d and I_{th} are 0.61 and 9.4 mA, respectively. Avoiding a drastic increase of I_{th}, R_f was determined as 5%. By 5% LR coating on the facet mirror, although I_{th} increases to 14.4 mA, η_d as high as 0.71 can be obtained.

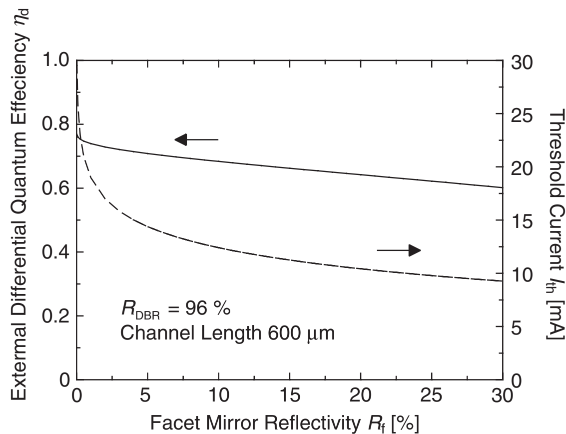

Fig. 3. Dependence of the external differential quantum efficiency and the threshold current on the reflectivity of the facet mirror.

Table I. Specifications of the fabricated curved-DBR laser.

Active Channel	Wavelength	960 nm
	Width	2.0 μm
	Length	600 μm
	Facet reflectivity	5%
Curved DBR Grating	DBR length	200 μm
	Grating period	153 nm
	Groove depth	70 nm
	Coupling coefficient	130 cm^{-1}
	Absorption loss	3 cm^{-1}
	Reflectivity	96%
	Wavelength bandwidth	1.6 nm

3. Device Fabrication

The specifications of the fabricated curved-DBR laser are summarized in Table I. The curved-DBR laser was fabricated using an MOVPE-grown strained-layer SQW-GRIN-SCH epitaxial structure, shown in Fig. 2. Selective area QW disordering was performed by rapid thermal annealing (RTA) using SiO_2 caps of different thicknesses.[4,5)] SiO_2 caps of 300-nm and 30-nm thickness were deposited by plasma chemical vapor deposition for the disordering and suppressing caps, respectively. Then RTA was performed at 860°C for 60 s and the both SiO_2 caps were removed by buffer etching.

After the evaporation of a Cr/Au p-electrode, the ridge structure was formed by reactive ion etching (RIE) in CH_4/H_2 gas using the electrode as a mask. The etch depth was accurately controlled by in-situ monitoring with a semiconductor laser probe using the etch-stop layer as a reference layer. The first-order curved DBR grating was fabricated by electron beam (EB) writing and two-step RIE. A thin SiO_2 layer was deposited and an EB resist was spin-coated. The DBR grating pattern (200-μm interaction length) with a 153-nm grating period was written by curved-scanning of the EB. The pattern was transferred to the SiO_2 layer by the first RIE in CF_4/H_2 gas and then transferred into the semiconductor layer to a depth of 70 nm by the second RIE in CH_4/H_2 gas. A benzocyclobutene (BCB) layer for electrical insulation was spin-coated. The planarized surface of the BCB layer was etched by RIE with CF_4/O_2 gas to open a self-aligned contact window. Following bonding electrode deposition, the BCB layer on the DBR grating region was removed by RIE to avoid a decrease of the reflectivity. After the wafer was thinned to 100 μm, an Au-Ge/Au n-electrode was evaporated on the backside. A facet mirror was formed by cleaving, and an Al_2O_3 LR layer with a thickness of 170 nm was evaporated on the cleaved facet to obtain 5% reflectivity. The device was soldered on a Cu heatsink. An SEM micrograph of the fabricated curved-DBR laser is shown in Fig. 4. For performance comparison, the curved-DBR laser without LR coating was also fabricated from the same wafer.

4. Experimental Results

The laser performance was measured under CW operation. The heatsink temperature was fixed at 15°C by a thermoelectric cooler. The dependence of the output power on the injection current for the curved-DBR laser with LR

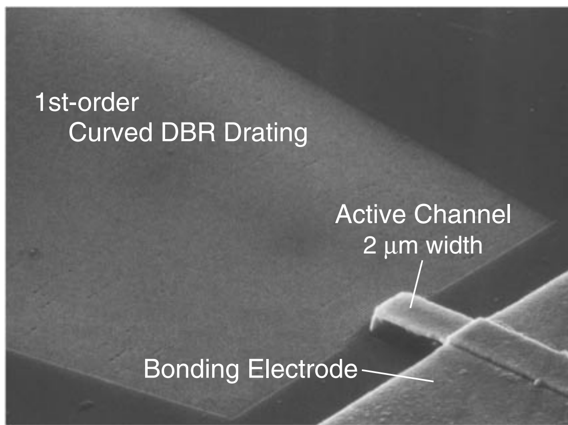

(a)

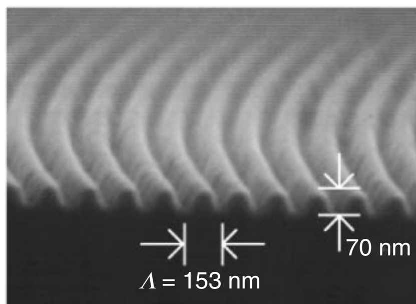

(b)

Fig. 4. SEM micrographs of (a) a perspective view of the fabricated curved-DBR laser and (b) a cross sectional view of the curved DBR grating.

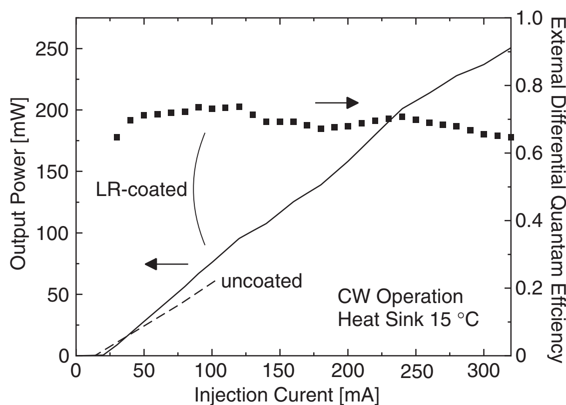

Fig. 5. Dependence of the output power and the external differential quantum efficiency on the injection current under CW operation. Dashed line shows the *L-I* characteristic for the curved-DBR laser without LR coating.

coating is shown in Fig. 5. The threshold current was 20 mA and the maximum output power of 251 mW was obtained. The dependence of the external differential quantum efficiency η_d on the injection current is also shown in Fig. 5. η_d as high as 0.74 was achieved above threshold up to 120 mA injection. Figure 6 shows the lasing spectrum at 100 mA injection. Single-mode lasing with a wavelength of 962 nm was obtained, and the linewidth was within the measurement resolution of 0.08 nm. As a result of adopting

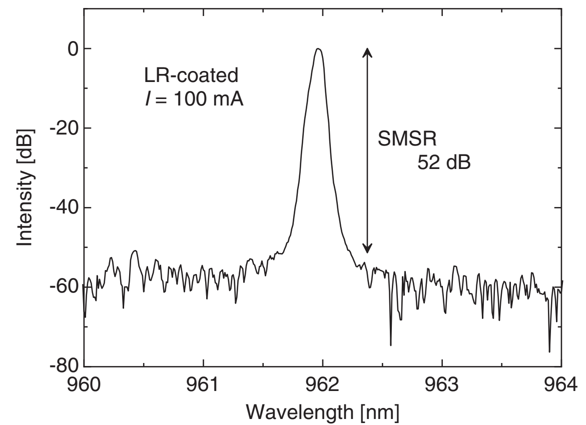

Fig. 6. Measured lasing spectrum at 100 mA injection for the curved-DBR laser with LR coating.

Table II. Comparison between the curved-DBR lasers with and without LR coating on the cleaved facet.

	LR-coated DBR laser	Uncoated DBR laser
Threshod current	20 mA	13 mA
External differential quantum efficiency	0.74	0.52
COD threshold	250 mW	90 mW

the first-order DBR grating and optimization of the coupling coefficient of the DBR, the side-mode suppression ratio (SMSR) of 52 dB was achieved. With increasing injection from 150 mA, the SMSR became worse gradually. The reason for degradation of the SMSR would be nonuniformity of Bragg wavelength over the DBR grating caused by the heat from the active channel and higher order lateral mode lasing. In order to obtain high SMSR even for higher injection, more efficient heat sinking, for example, adopting Au-Sn solder and junction down mounting, is required.

To confirm the effect of LR coating on the facet mirror, light-current (*L-I*) characteristic for the curved-DBR laser without coating was measured (dashed line in Fig. 5). Table II shows the comparison between the fabricated curved-DBR lasers with and without LR coating on the facet mirror. By LR coating, I_{th} was increased to 20 mA and η_d was enhanced to 0.74, which is close to the estimated value of 0.71. COD resistivity was highly improved. These results confirm the effectiveness of the Al_2O_3 LR coating on the facet mirror.

Balanced detectors were used to measure the intensity noise relative to the standard quantum limit (SQL).[7,8] A half-wave plate and polarization beam splitter were used to divide the optical power equally between two Si PIN photodiodes, as shown in Fig. 7. The sum and difference of the two photodiode output signals, corresponding to the intensity noise of the laser under test and the SQL reference level, respectively, were displayed alternately on an RF spectrum analyzer. Taking into account of all optical losses of the measurement system, the total quantum efficiency was estimated as $\eta_{det} = 0.73$. Figure 8 shows the measured noise spectrum. The curved-DBR laser with LR coating was used

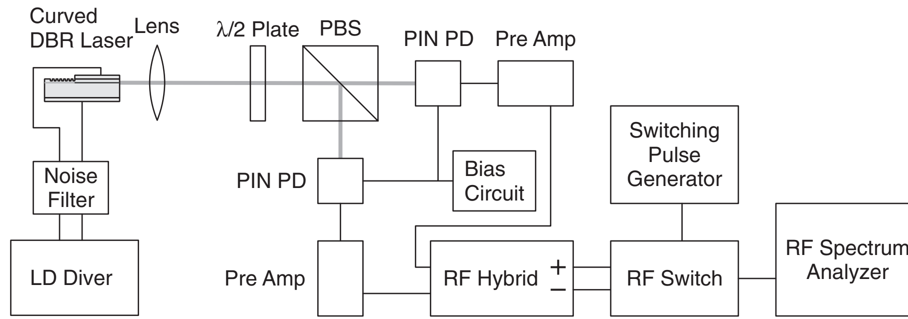

Fig. 7. Experimental Setup for noise measurement using balanced detectors.

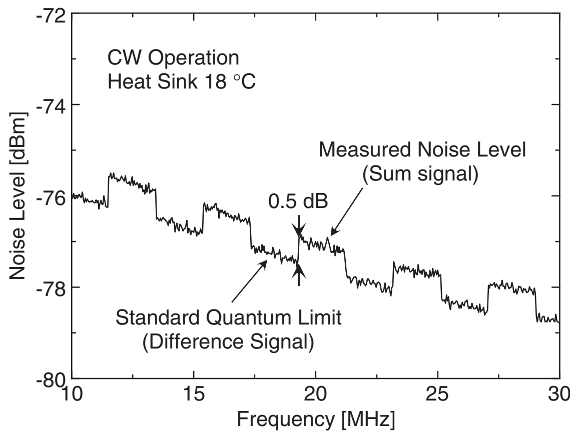

Fig. 8. Noise spectrum relative to the standard quantum limit measured by balanced detectors.

at an injection current of 100 mA. Figure 8 shows that the laser noise level for a frequency range between 10 and 30 MHz is about 0.5 dB above the SQL level. Compensation for the detection efficiency by using $S_{\rm mes} = \eta_{\rm det} S + (1 - \eta_{\rm det})$ gives a result that the laser intensity noise level S is 0.7 dB above the SQL level. The reason for such low noise characteristic is the high $\eta_{\rm d}$, the low threshold and the high SMSR. If the quantum efficiency is not very high, the spontaneous emission and/or nonradiative recombination give rise to excess noise over the SQL. Such excess noise is reduced in the present laser of high quantum efficiency. A very high SMSR is also an important requirement to avoid the mode partition noise.

5. Conclusions

An InGaAs quantum well curved-DBR laser was designed for high efficiency and high wavelength purity operation and fabricated by a simple process without regrowth. The quantum well was selectively disordered in the DBR grating region to accomplish low propagation loss. As a result of optimization of the curved DBR grating and low-reflection coating on the facet mirror, single-mode lasing with an external differential quantum efficiency as high as 0.74 and a side mode suppression ratio of 52 dB was achieved. Low noise characteristic of 0.7 dB above the standard quantum limit was obtained.

Acknowledgements

This work was supported in part by Grants-in-Aid for Scientific Research from the Ministry of Education, Culture, Sports, Science and Technology (MEXT), and Handai Frontier Research Center (FRC).

1) M. Uemukai, A. Yoshimoto, N. Matsumoto, T. Suhara, H. Nishihara, N. Eriksson and A. Larsson: Electron. Lett. **33** (1997) 1464.
2) M. Uemukai, N. Matsumoto, T. Suhara, H. Nishihara, N. Eriksson and A. Larsson: IEEE Photon. Technol. Lett. **10** (1998) 1097.
3) M. Uemukai, M. Miyata, N. Shimada, T. Suhara, H. Nishihara, N. Eriksson, P. Modh and A. Larsson: Jpn. J. Appl. Phys. **39** (2000) 1503.
4) N. Shimada, Y. Fukumoto, M. Uemukai, T. Suhara, H. Nishihara and A. Larsson: Jpn. J. Appl. Phys. **39** (2000) 5914.
5) N. Shimada, Y. Fukumoto, M. Uemukai, T. Suhara, H. Nishihara and A. Larsson: IEEE J. Select. Top. Quantum Electron. **7** (2001) 350.
6) N. Eriksson, M. Hagberg and A. Larsson: IEEE J. Quantum Electron. **32** (1996) 1038.
7) S. Machida, Y. Yamamoto and Y. Itaya: Phys. Rev. Lett. **58** (1987) 1000.
8) M. J. Freeman, H. Wang, D. Steel, R. Craig and D. Scifres: Opt. Lett. **18** (1993) 2141.